Influence of topography and Co domain walls on the magnetization reversal of the FeNi layer in FeNi/Al_2O_3/Co magnetic tunnel junctions

Fabien Romanens, Jan Vogel, Wolfgang Kuch, Keiki Fukumoto, Julio Camarero, Stefania Pizzini, Marlio Bonfim, Frédéric Petroff

Influence of topography and Co domain walls on the magnetization reversal of the FeNi layer in $FeNi/Al_2O_3/Co$ magnetic tunnel junctions

F. Romanens,[1] J. Vogel,[1] W. Kuch,[2] K. Fukumoto,[2] J. Camarero,[3] S. Pizzini,[1] M. Bonfim,[1] and F. Petroff[4]

[1] *Laboratoire Louis Néel, CNRS, 25 avenue des Martyrs, BP 166, F-38042 Grenoble cedex 9, France*
[2] *Institut für Experimentalphysik, Freie Universität Berlin, Arnimallee 14, D-14195 Berlin, Germany*
[3] *Dpto. Física de la Materia Condensada, Universidad Autónoma de Madrid, E-28049 Madrid, Spain.*
[4] *Unité Mixte de Physique CNRS/Thales, Route départementale 128, F-91767 Palaiseau cedex, France*

(Dated: October 5, 2006)

We have studied the magnetization reversal dynamics of $FeNi/Al_2O_3/Co$ magnetic tunnel junctions deposited on step-bunched Si substrates using magneto-optical Kerr effect and time-resolved x-ray photoelectron emission microscopy combined with x-ray magnetic circular dichroism (XMCD-PEEM). Different reversal mechanisms have been found depending on the substrate miscut angle. Larger terraces (smaller miscut angles) lead to a higher nucleation density and stronger domain wall pinning. The width of domain walls with respect to the size of the terraces seems to play an important role in the reversal. We used the element selectivity of XMCD-PEEM to reveal the strong influence of the stray field of domain walls in the hard magnetic layer on the magnetic switching of the soft magnetic layer.

PACS numbers: 75.60.Jk, 75.60.Ch, 75.70.-i, 85.70.Kh

I. INTRODUCTION

Magnetic tunnel junctions and spin valves are extensively used in magnetic storage devices, and are also interesting from a fundamental point of view. Their active part, composed of two ferromagnetic (FM) materials with different coercivities separated by a non-magnetic (NM) spacer layer, presents a number of interesting phenomena like giant magnetoresistance[1,2] and spin transfer torque.[3,4] In these trilayer systems, magnetostatic effects can strongly influence the magnetization reversal. For instance, an interaction between the two magnetic layers can be induced by correlated roughness at the FM/NM interfaces. This roughness induces magnetic charges at the interfaces, and the interaction between them leads to the so-called "orange-peel" coupling,[5] favoring a parallel alignment of the magnetization of the two ferromagnetic layers. The roughness also influences the domain wall pinning and therefore the magnetization reversal. In a previous paper,[6] we have revealed the effect of modulated roughness, induced by deposition on step-bunched Si substrates, on the magnetization reversal and coupling in magnetic trilayers. Steps with an orientation perpendicular to the easy magnetization axis are at the origin of a strongly localized orange-peel coupling.[6] On the other hand, steps parallel to the easy magnetization axis induce strong demagnetizing effects when domain walls are located on these steps. This causes a pinning of the domain walls that hinders reversal by domain wall propagation. One might expect this effect to be particularly important when the difference in energy between domain walls situated on and situated between steps is large. To test the influence of the topography on the magnetization reversal, we have investigated FM/NM/FM trilayers deposited on step-bunched substrates with different miscut angles, leading to different widths of the terraces and thus to different distances between steps. We have used magneto-optical Kerr effect and time-resolved x-ray magnetic circular dichroism combined with photoemission electron microscopy (XMCD-PEEM) to obtain both a global and a detailed microscopic view of the influence of the substrate-induced layer topography on the magnetization reversal. These measurements show that in the samples with the largest terraces nucleation of reversed domains is easier while the pinning of domain walls is stronger than in samples with smaller terraces. In order to explain this we suggest that the width of domain walls with respect to the average width of terraces has to be taken into account.

Apart from magnetostatic effects induced by layer topography, stray fields from inhomogeneously magnetized regions in one of the layers can also influence the static and dynamic magnetic properties of the other layer. For example, domain walls in the soft magnetic layer can create stray fields that are large enough to influence the magnetization of the hard magnetic layer in soft FM/NM/hard FM trilayers, as shown by Thomas *et al.*[7] More recently, several authors have shown direct evidence of the effect of a domain wall in one layer on the static magnetic configuration of the other layer.[8,9,10,11] In a recent paper,[12] we have used the element selectivity of XMCD-PEEM to study independently the magnetization of both magnetic layers in $FeNi/Al_2O_3/Co$ trilayers, showing that domain walls in the hard magnetic layer locally decrease the nucleation barrier for the switching of the soft magnetic layer. In this paper, we have extended this study in order to obtain information on the relative influence of topography and domain wall stray fields on the nanosecond magnetization reversal in spin-valves and magnetic tunnel junctions.

II. EXPERIMENTAL METHODS

The samples studied were $Fe_{20}Ni_{80}$(4 nm)/ Al_2O_3 (2.6 nm)/ Co(7 nm)/ CoO(3 nm) magnetic tunnel junctions deposited on Si(111) substrates by RF sputtering. The CoO layer was used to increase the coercive field of the Co layer. In fast dynamic measurements, coercivities increase and the field range over which the magnetization reverses (magnetization transition) is broader than in quasi-static conditions.[6] A large difference in quasi-static coercivity between the two magnetic layers is therefore needed in order to allow the FeNi magnetization to be switched without changing the Co magnetization in our fast dynamic measurements.

Three different samples (named samples I, II, and III) were deposited on substrates with miscut angles along the $[11\overline{2}]$ direction of 4°, 6°, and 8° respectively. After annealing, all the substrates present a step-bunched surface with ellipsoidal terraces.[13] Transmission electron microscopy images show that these topographic features are well reproduced by the subsequently deposited layers.[6] The size of the terraces and the height of the steps depend on the miscut angle (for a miscut angle of 4, 6 and 8°, the average terrace width is about 60, 40, and 20 nm, and the step height is about 5, 4, and 3 nm respectively). The steps make an angle of about 60° with respect to the normal of the surface (see Fig. 1 in Ref[6]). This topography induces a uniaxial in-plane magnetic anisotropy in all three samples, with the easy axis parallel to the long axis of the terraces.

We have studied the magnetization reversal of these samples using Kerr magnetometry and XMCD-PEEM. Longitudinal Kerr effect measurements were performed by illuminating the samples with a linearly polarised He-Ne laser beam. The polarization rotation of the reflected light due to the Kerr effect is detected by a combination of a Wollaston prism and a pair of photodiodes. For "slow" magnetization reversal (for a field sweep rate dH/dt below 10 T/s) the field was applied using a ferrite electromagnet. For "fast" magnetization reversal, "strip-line" coils made of a hairpin-shaped copper ribbon into which the samples were inserted was used. A window was opened in the top part of the coil in order to allow illumination.[14] These coils, in combination with a fast current generator, allow magnetic fields up to 20 mT to be generated, with a rise-time of the order of 10 ns. The error bar on the field values obtained with this coil, given in the text and figures, is estimated to be about 10%. Kerr magnetometry allows macroscopic magnetization reversal to be measured for a wide range of time scales (from quasi-static to the nanosecond timescale). However it does not give local information about the magnetic switching as it measures the sample's magnetization integrated over the laser spot size, which was about 100 μm in our measurements.

In order to obtain local information, we have performed magnetic imaging using time resolved XMCD-PEEM with the coil mentioned above. These measurements were carried out at beamlines UE56-2 and UE52 of the BESSY synchrotron in Berlin. The sample is illuminated with circularly polarized x-rays. The XMCD mechanism causes the x-ray absorption of the sample to depend on the relative orientation of the local magnetization and the helicity vector of the x-rays.[15,16] Absorption of x-rays creates photo-emitted electrons with an intensity that is proportional to the local absorption. These electrons are collected by an electron microscope and projected on a CCD camera, therefore allowing to form an image of the sample in which the intensity represents the projection of the local magnetization on the direction of the x-ray propagation.[17,18] In order to enhance the magnetic contrast and subtract the topographic component, the final image is the difference between images taken with right and left circularly polarized x-rays. One powerful feature of this technique is its element selectivity, i.e. by tuning the photon energy to the Fe L_3 or Co L_3 absorption edge, the permalloy or cobalt layer magnetization can be probed independently. When applying a magnetic field on the sample, the trajectory of the photo-emitted electrons is changed, leading to a shift of the image. In order to correct this shift, we have translated the images in Fig. 5-7 so that the same region of the sample is shown on each image independently on the applied field.

Temporal resolution was obtained by exploiting the time-structure of synchrotron radiation. In the single bunch operation mode of BESSY, photon pulses are emitted with a repetition rate of 1.25 MHz. The temporal resolution of our measurements, defined by the width of the photon pulses (∼70 ps) and electronic jitter, was better than 100 ps. Measurements were performed in pump-probe mode, by synchronizing the photon pulses with the applied field pulses.[19,20] By tuning the delay between the photon pulse and the magnetic field, magnetization reversal was studied as a function of time during the magnetic pulse.

III. MAGNETIZATION REVERSAL

The quasistatic hysteresis loops for the three samples obtained using longitudinal Kerr effect measurements are shown in Fig. 1. The hysteresis loops were recorded with the magnetic field applied along the long axes of the terraces, corresponding to the easy magnetization axis. Because of the presence of the CoO layer, the coercive field of the Co layer is much larger than the coercive field of the FeNi layer, thus leading to well defined FeNi minor loops. These FeNi minor loops are not centered on zero-field due to the so-called Néel "orange peel" coupling between the two magnetic layers. This magnetostatic coupling, due to the presence of steps between terraces, has been previously studied, and its manifestation depends on the switching mode of magnetization.[6]

The roundness of the FeNi minor loop for sample I indicates that domain nucleation plays an important role

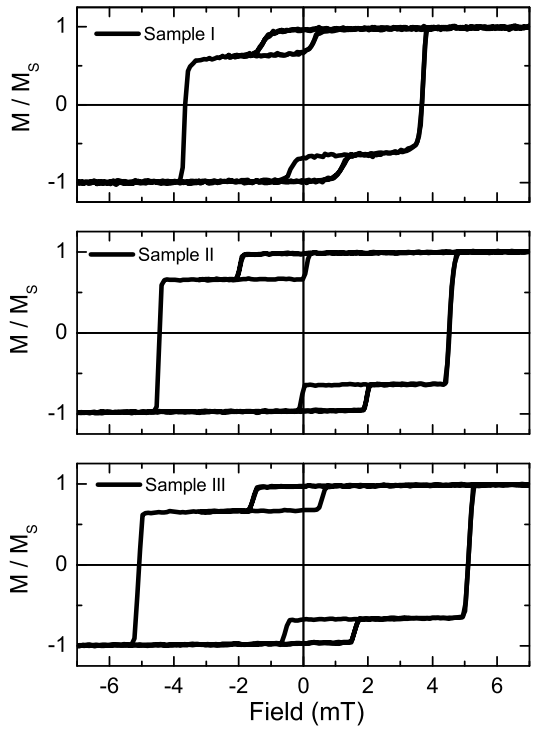

FIG. 1: Quasistatic hysteresis loops and minor loops for magnetic tunnel junctions deposited on step-bunched Si with a miscut angle of 4^o (top), 6^o (middle) and 8^o (bottom). The hysteresis loops are taken with the magnetic field applied along the easy magnetization axis (parallel to the long axis of the substrate terraces).

in the reversal of this sample, and that domain walls are strongly pinned. The hysteresis loops of sample II and III are square shaped. This indicates that the coercive fields of these samples are determined by the field needed to nucleate domains and that once a domain is nucleated, magnetization reversal takes place by fast propagation of domain walls. The transitions in the minor loop of sample III are more tilted than for sample II. The loops in Fig. 1 are averages over several (some tens) of single hysteresis loops. For sample sample III, we observed a distribution of reversal fields, probably due to different nucleation positions and therefore different times/fields for which a domain wall crosses the laser spot. In the averaged loops, the FeNi magnetization transition therefore appears less square.

We have measured hysteresis loops with field sweep rates ranging from 10 mT/s to 1 kT/s. The permalloy coercive field as a function of dH/dt is plotted in Fig. 2. The coercive field was taken as the average of the positive and negative reversal fields of the minor hysteresis loops. When increasing the applied field sweep rate, dynamic effects appear such as an increase of the coercive field and a broadening of the magnetization transitions.

For the lowest field sweep rates, the increase of the permalloy coercive field is quite linear with the logarithm

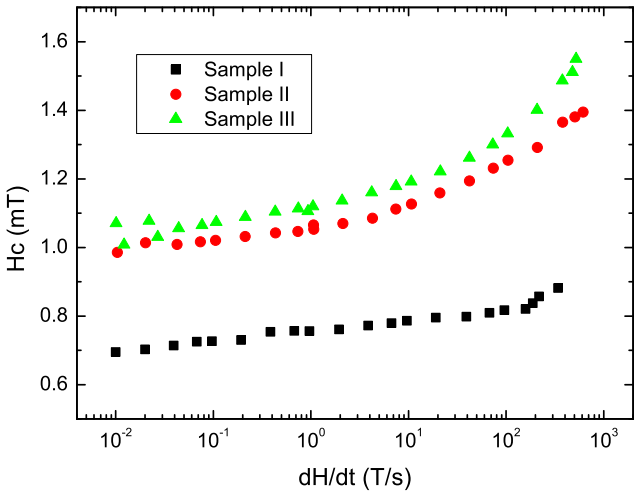

FIG. 2: Coercive field of the $Fe_{20}Ni_{80}$ layer as a function of the applied field sweep rate dH/dt.

of the applied field sweep rate as expected from theory.[21] In a previous work,[22] a clear deviation from this linear regime at fast sweep rates was interpreted as a transition from a propagative reversal at low sweep rates to a more nucleative reversal at fast timescales, as suggested by Raquet.[23] In our case, for sample I a deviation from linearity is well observed at a sweep rate of 100 T/s, but the shape of the quasistatic hysteresis loop indicates that even at very low sweep rates nucleation already plays an important role in the magnetization reversal. The observed transition can, however, be due to a sudden increase of the nucleation density at high field sweep rates. For samples II and III, no clear transition is visible in the investigated range of field sweep rates. This means that either there is no critical field at which a sudden transition from domain wall propagation to nucleation dominated reversal takes place, or that this critical field falls outside the measured range. However, the interpretation of the $H_c(dH/dt)$ data is difficult and not clear enough to conclude on the mechanisms governing the magnetization reversal.

For a better understanding of these mechanisms, we have carried out measurements of magnetization relaxation at the nanosecond timescale. Magnetization relaxation has been used in Co/Pt[24] and other systems where domain wall pinning is important. The advantage of relaxation measurements with respect to measurements with varying field sweep rates is that the magnetic field is fixed during the magnetization reversal. In planar thin films, the reversal is very fast, thus relaxation measurements on our samples were possible only for very fast risetimes of the magnetic field. In our magnetization relaxation measurements, the samples were initially saturated in the positive direction using a quasi-static magnetic field. A negative field pulse was then applied at $t = 0$ along the easy magnetization axis (see dotted lines in Fig. 3), with an amplitude sufficient to reverse

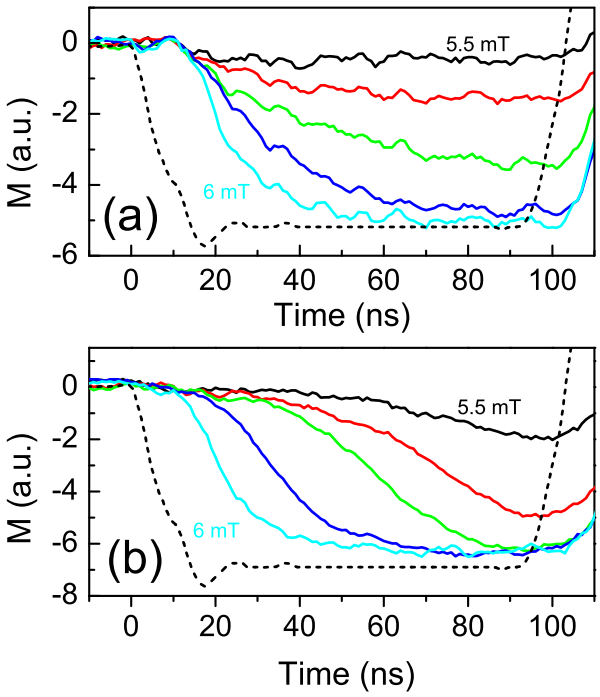

FIG. 3: Fast magnetization relaxation for sample II (a) and sample III (b). The magnetization decay is plotted in solid lines for different applied field values between 5.5 and 6 mT. The shape of the magnetic field pulse for a pulse with an amplitude of 6 mT is shown as the dashed line. A synchronous noise can be seen in (a). This noise is due to electromagnetic interference created by the current generator and the coil.

the permalloy magnetization but low enough so that the cobalt magnetization did not change. After the 100 ns long negative field pulse, a positive pulse (not shown in Fig. 3) was applied in order to saturate the permalloy magnetization again in the positive direction. The field was applied with a rise time of about 10 ns, and the amplitude of the field was small enough for the reversal to take place mainly during the plateau in which the field was constant. Due to the small barrier for nucleation of reversed domains in sample I, the magnetization of this sample always started reversing before the field plateau. In Fig. 3, only the relaxation curves for sample II and sample III are therefore shown. Each curve in Fig. 3 is an average over about 500 relaxation curves, to increase the signal to noise ratio.

It can be seen in Fig. 3 that the field needed to reverse the permalloy layer (against the direction of the Co magnetization) in 100 ns is about 5.7-5.9 mT. This is a factor 2-3 higher than for the quasi-static measurements. This value is in agreement with the fast increase of coercivity expected from an extrapolation of the curves in Fig. 2 (5-6 mT in 100 ns gives an average dH/dt of 5-6$\times 10^4$ T/s). A similar behavior has been observed for Co/Pt systems[25].

Oscillations due to precessional-like magnetization reversal have been observed in several micrometer-sized thin film structures[26,27,28,29]. In these structures, the zero-field ground state is a flux-closure domain state due to finite-size and demagnetizing field effects, which also have an important influence on the magnetization dynamics. They play no significant role in the magnetization dynamics of our samples, consisting of in-plane magnetized continuous films for which homogeneous magnetization along the easy axis gives the lowest energy. In that case, the magnetization reversal occurs through incoherent nucleation and propagation processes that are not expected to give rise to oscillations in the magnetization behavior. The oscillations observed in the relaxation curves of Fig. 3, especially for sample II, are due to synchronous noise, caused by the electromagnetic interference between the pulsed current generator and the magnetic coil.

Both sets of relaxation curves can be understood by the model initially developed by Fatuzzo for ferroelectric materials[30] and later adapted to ferromagnetism by Labrune.[31] According to this model, the relaxation curve is exponential in the case of nucleation-dominated reversal, and S-shaped in the case of propagation-dominated reversal. A clear difference between the behavior of the two samples is observed in these fast relaxation measurements. Sample II has a quasi exponential relaxation, indicating more nucleation than in sample III which has an S-shaped relaxation curve. Even if there are no significant differences in the hysteresis loops nor in the $Hc(dH/dt)$ data, these relaxation measurements indicate that, at these short timescales, the reversal is more propagative in sample III than in sample II.

In summary, magnetometry measurements indicate that nucleation plays an important role in the reversal of sample I, whereas domain wall propagation dominates the reversal of sample II and III in quasistatic conditions. During faster reversal, the nucleation becomes more important in the magnetization reversal of sample II, indicating a change of regime compared to quasistatic conditions. For sample III, domain wall propagation is still the process dominating the reversal even at short timescales.

In order to confirm these conclusions with microscopic measurements, we have performed time-resolved XMCD-PEEM measurements. Figure 4 shows the evolution of the domain structure of the permalloy layer during the application of a magnetic pulse applied along the easy axis of magnetization. The trilayer is initially saturated in one direction, giving a black image. In this condition, permalloy and cobalt magnetizations are parallel. At time $t = 0$ the magnetic pulse triggers magnetization reversal of the permalloy layer toward antiparallel alignment with Co. The reversal occurs by nucleation of reversed domains, which appear as white contrast in Fig.4, and a subsequent propagation of domain walls.

The images clearly show that for similar field values the number of nucleated domains strongly decreases going from sample I to sample III. Actually, the main part of the reversal in sample I takes place during the rise-time of the field pulse, while the dynamics of the domain

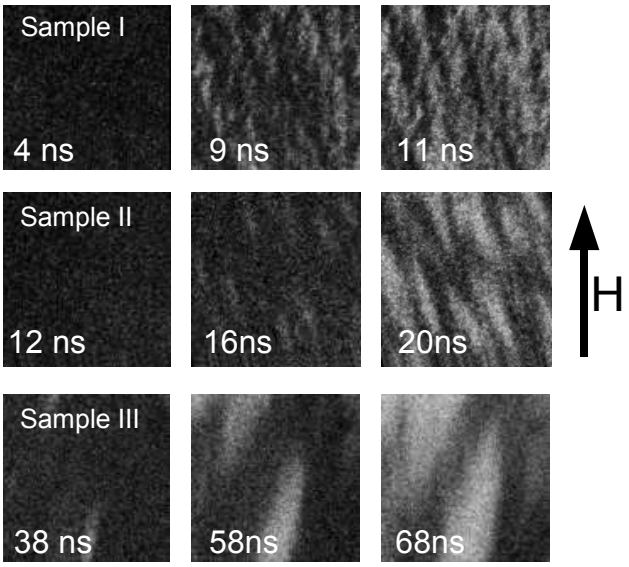

FIG. 4: Magnetization reversal of the FeNi layer in the different FeNi/Al_2O_3/Co trilayers. The applied magnetic field is about 6.5 mT for sample I (top row) and sample II (middle row), and about 6 mT for sample III (bottom row). The projection of the x-ray incidence direction on the sample surface is pointing up in the images (parallel to the arrow) and is parallel (anti-parallel) to the direction of the field for positive (negative) pulses. The magnetization direction is in the plane of the layers and points up (parallel to the arrow) for black domains, and down for white domains. The time delay with respect to the beginning of the (negative) magnetic pulse is indicated in the images. The field of view is about 50 μm for all the images.

walls at the plateau is very slow. In sample III the density of nucleated domains is very small, and the images for this sample are quite blurred. Note that the images are acquired in a pump-probe mode, averaged over about 10^8 magnetic and photon pulses. The blurred images of sample III therefore indicate that the domain wall motion that dominates the reversal in this sample is less reproducible than domain nucleation. A wide distribution of nucleation barrier energies seems to exist in these samples, which is also indicated by the strong increase of the number of nucleated domains upon increasing pulse height.[32] The nucleation is therefore mainly field induced and thermal activation plays a minor role.

We conclude that both macroscopic magnetometry and microscopic magnetic imaging measurements indicate that the reversal mechanism for the FeNi/Al_2O_3/Co trilayers depends on their topography. While the nucleation density decreases going from sample I (larger terraces) to sample III (narrower terraces), the domain wall mobility increases and domain wall pinning therefore decreases.

We propose the following explanation for these results. The energy of a domain wall will depend on whether it is on a terrace or on a step. In these thin films (thickness <10 nm), domain walls are of the Néel-type.[33] If located on a step parallel to the easy magnetization axis, the magnetization in the center of the domain wall will point in the direction perpendicular to the step leading to strong demagnetizing fields and therefore to a large domain wall energy. In a previous paper,[6] we have confirmed that using micromagnetic simulations. Energetically it is therefore favorable for the domain walls to be situated on the flat terraces. This is however only possible if the terraces are larger than the domain wall width. For the smaller miscut angle (sample I), the terraces are about 60 nm large and the reversal is found to occur mainly by nucleation. A typical domain wall width in permalloy is one hundred nanometers, but some authors have shown that domain wall width is decreased when the wall is on a step.[34] Also our simulations[6] have shown that a domain wall can be confined on a terrace by a slight compression of its width. In sample I, a domain wall can therefore "fit" on a terrace and the energy cost to create a domain wall is relatively small. However, in order to propagate it will have to overcome a step. This leads to a stronger domain wall pinning and consequently a magnetization reversal with mainly nucleation. On the contrary, for samples II and III the terraces are smaller than the domain wall width in permalloy. A domain wall in these samples will therefore be partly located on one or more steps, leading to a higher barrier for domain nucleation. However, once nucleated the domain walls can propagate quite easily since the extra energy barrier for passing another step is rather small. Moreover, the step heights for sample II and even more sample III are also smaller than for sample I. The reversal in these samples will therefore mainly take place by propagation.

IV. INFLUENCE OF DOMAIN WALLS

In the previous section we have shown that the magnetization reversal in the soft magnetic layer of magnetic tunnel junction-like trilayers depends on topography. In this section we will show that also inhomogeneities in the magnetization of the hard layer, like the presence of magnetic domain walls, can influence the magnetization reversal of the soft layer. In a previous paper[12], we have shown that a domain wall in the Co layer of sample II locally decreased the barrier for domain nucleation in the FeNi layer. We have performed time-resolved XMCD-PEEM measurements also on the other samples, in order to confirm that the preferential nucleation induced by domain wall stray fields is a general property of this type of trilayers. The effect of domain wall stray fields on the magnetization reversal should be larger for samples with a higher intrinsic barrier for domain nucleation. This nucleation barrier strongly depends on topography as shown in the previous section.

The results for the three different samples are shown in Figs. 5 to 7. A domain structure is initially created in the Co layer by applying a 3 ms long magnetic pulse of about 3 mT. The domain structure of the Co layer is

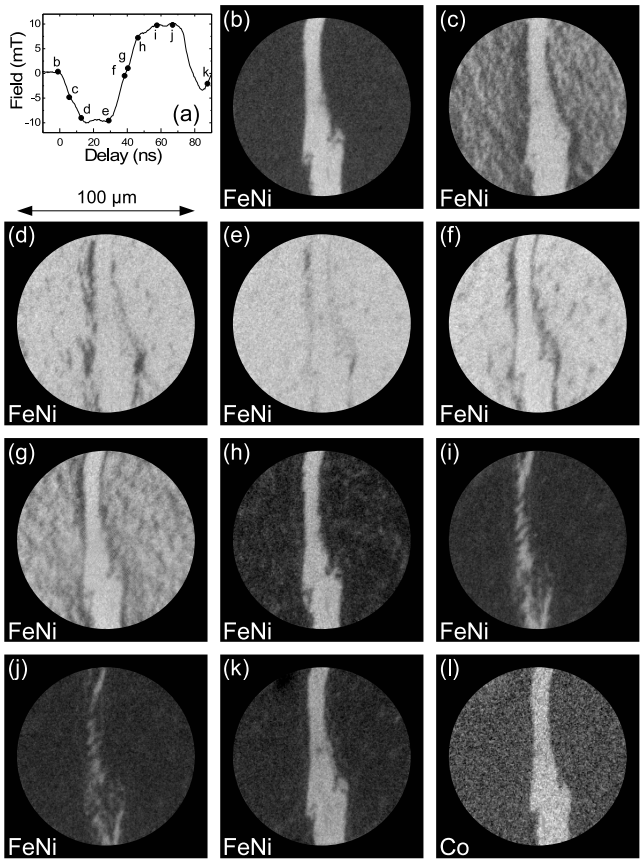

FIG. 5: Time-resolved PEEM images for sample I (4° miscut angle). (a) Bipolar applied magnetic field pulses. (b) to (k) FeNi domain structure for different delays between magnetic field and photon pulses as indicated in (a). (l) Co domain structure. The directions of incoming photons, applied field and local magnetization are the same as in Fig. 4. The field of view for each image is 100 μm.

shown in Figs. 5(l), 6(l) and 7(l) for sample I, II and III respectively. Fast bipolar magnetic field pulses, shown in Figs. 5(a), 6(a), and 7(a), are then applied to the sample. The applied field is strong enough to reverse the permalloy magnetization. Note that even if this field is higher than the quasistatic cobalt coercive field, the pulse duration is too short to change the cobalt domain structure (as checked by imaging the Co magnetization at different times during the magnetic pulse). The magnetization reversal of the permalloy layer is shown in images (b) to (k). Secondary electrons generated in the Co layer are attenuated by the FeNi layer on top, leading to a smaller signal to noise ratio for images of the Co domain structure.

For sample I, Fig. 5(b) shows that, before the magnetic field pulse, the FeNi domain pattern is the same as that of the Co layer. This is a consequence of the "orange-peel coupling" which favors parallel alignment of the two layers' magnetizations. From Figs. 5(b) to 5(d), the positive magnetic field reverses the black regions of the FeNi layer, and the reversal occurs by nucleation of many white domains. At the end of the positive field pulse (Fig. 5(e)), the FeNi layer is almost fully saturated, except a gray region which seems to be correlated to the position of the Co domain walls. At the beginning of the negative field pulse, Fig. 5(f) shows some fuzzy black spots which correspond to nucleation of new domains, as well as two black lines which correspond to domains which were still present at the end of the first pulse. The FeNi region on top of black Co domains is the first to be reversed as shown in Fig. 5(g), and this reversal takes place with a high nucleation density. The negative field pulse is not sufficient to fully saturate the FeNi layer (Figs. 5(i) and (j)). The field overshoot leads to a FeNi domain structure similar to that of the Co layer as shown in Fig. 5(k).

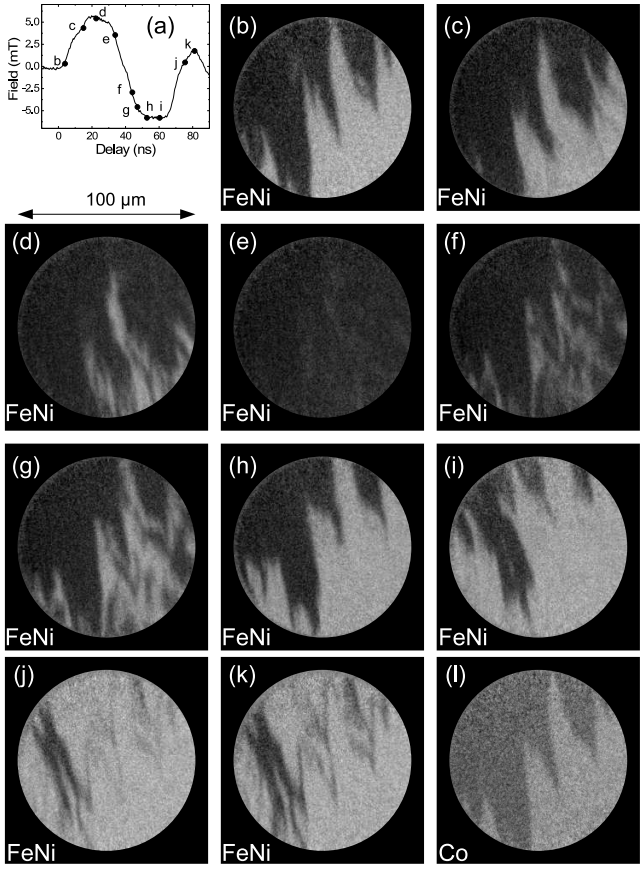

FIG. 6: Time-resolved PEEM images for sample II (6° miscut angle). (a) Bipolar applied magnetic field pulses. (b) to (k) FeNi domain structure for different delays between field pulse and photon pulses as indicated in (a). (l) Co domain structure. The directions of incoming photons, applied field and local magnetization are the same as in Fig. 4. The field of view for each image is 100 μm.

Figure 6 shows the magnetization dynamics of sample II's permalloy layer. The Co domain structure, which is unchanged by the magnetic pulse, is shown in 6(l). The reversal of the FeNi layer is more propagative than for sample I (Figs. 5(c), (d) and (f) to (i)), confirming the conclusions of the previous section. At the end of the two

magnetic field pulses, the FeNi layer is almost fully saturated, except for some faint lines at the same position as the domain walls in Co, which are visible in Figs. 6(f) and (j). One can clearly see in Figs. 6(f) and (k) that the reversal is easier above the Co domain wall. Reversal is in general favored where the coupling and the applied field are parallel but the domains which grow on top of the Co domain wall are larger than elsewhere in the sample. This means that the reversal on top of the domain walls has started first. After the negative field pulse, the positive overshoot make the FeNi domain structure again similar to that of the Co layer (not shown in Fig. 6).

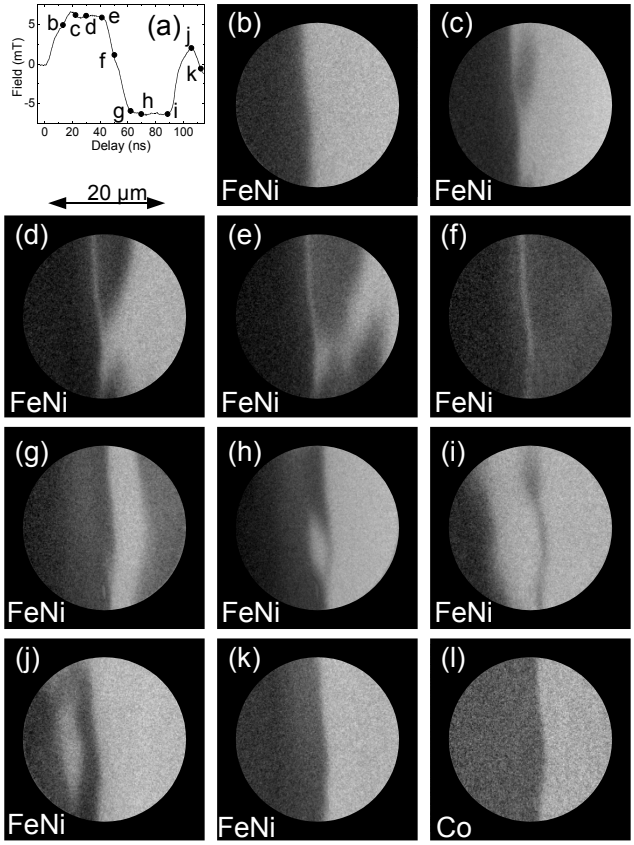

FIG. 7: Time-resolved PEEM images for sample III (8° miscut angle). (a) Bipolar applied magnetic field pulses. (b) to (k) FeNi domain structure for different delays between field pulse and photon pulses as indicated in (a). (l) Co domain structure. The directions of incoming photons, applied field and local magnetization are the same as in Fig. 4. The field of view for each image is 20 μm.

Figure 7 shows the magnetization dynamics of sample III with a smaller field of view and a better spatial resolution ($\simeq 0.3$ μm) than Figs. 5 and 6. In this series of images, it can be clearly seen that the region of the FeNi layer above the Co domain wall is hard to saturate. At the end of the positive field pulse, Fig. 7(f) shows a gray line that corresponds to the position of the Co domain wall. Also in Fig. 7(i), at the end of the negative pulse, a gray line is visible at the same position. This means that a "quasi-wall" stays present in the FeNi layer even for applied magnetic fields up to 6 mT. It is interesting to note that the pulse length of 40 ns is apparently too short to make the Co domain wall move, even if the field amplitude is well above the Co quasistatic coercive field. This also means that the effect of strong fields on the 'quasi-wall' without moving the Co domain wall can only be studied in these fast dynamic measurements. On the other hand, we can not completely be sure that the gray zone in Figs. 7(f) and (i) corresponds to a single quasi-wall and not to an accumulation of several 360° domain walls with a width smaller that the spatial resolution of the images. Even more than in the other two samples, the preferential nucleation above the Co domain wall is particularly clear in sample III. This is due both to the smaller field of view and the zoom-in on the domain wall and the domination of domain wall propagation in the reversal of this sample. The difference in energy barrier for nucleation between the region above the Co domain wall and other regions in the sample is therefore larger. A sweeping displacement of the domain walls starting from the Co domain wall is clearly seen both in Figs. 7(c)-(e) for white-to-black reversal and in Figs. 7(h)-(i) for black-to-white reversal. In Fig. 7, we do not show exactly the same part of the sample in all the images in order to keep the field of view maximum. This allows a better visualisation of the sweeping domain wall displacement. We have checked, however, that the central region in the FeNi images always corresponds to the domain wall position in the Co layer.

For all three samples we studied, the presence of domain walls in the hard magnetic layer makes it difficult to saturate the soft layer. This effect can be understood by taking into account the domain wall stray field. In our previous paper,[12] we have discussed the effect of this stray field. In particular, micromagnetic simulations have shown that the Co domain wall stray field is sufficient to create a region where the FeNi magnetization is tilted away from the easy axis, creating a so-called quasi-wall. When applying a magnetic field parallel to the easy axis, the torque induced by the field on the magnetic moments is higher in this quasi-wall than elsewhere in the sample, leading to an easier nucleation above the Co domain walls. This effect is most clearly visible for sample III with the narrowest terraces. In this sample, the difference between nucleation barriers for domain reversal with and without domain wall in the Co layer is largest. Moreover, once nucleated, the domain wall propagation is easiest in this sample. In sample I, domain wall propagation is strongly pinned, and even if preferential nucleation still seems to take place above Co domain walls, this nucleation does not lead to an easier and faster switching of the FeNi layer magnetization like in sample III.

V. CONCLUSION

We have used time-resolved Kerr effect measurements and time-resolved XMCD-PEEM imaging to study the nanosecond layer-resolved magnetization dynamics of FeNi/Al_2O_3/Co trilayers deposited on step-bunched Si(111) substrates. We have revealed a strong dependence of the fast magnetic switching on the layer topography. The phenomenon dominating magnetic switching (domain nucleation or domain wall propagation) strongly depends on the average width of the substrate terraces and the height of the steps between terraces. For relatively large terraces of 60 nm separated by 5 nm high steps, domain nucleation is dominating while domain propagation is strongly pinned. On the other hand, for terraces with a width of only 20 nm separated by 3 nm high steps, domain wall propagation dominates over domain nucleation. We propose that this difference can be explained by taking into account the domain wall width. While a (compressed) domain wall can fit a single 60 nm terrace, it will extend over one or more steps for 20 nm wide terraces. The minimum domain wall energy will therefore be smaller for 60 nm wide terraces, but the energy barrier for crossing a step will be larger. Coercivity measurements as a function of applied magnetic field sweep rate and magnetization relaxation measurements can give an indication of the magnetization reversal mechanisms and their evolution as a function of time and applied field. However, our results clearly show that for a comprehensive picture of fast magnetic switching a microscopic technique is needed. Using the element selectivity of time-resolved XMCD-PEEM, we have revealed the influence of stray fields emerging from domain walls in the hard magnetic layer on the magnetic switching of the soft magnetic layer. These stray fields locally decrease the barrier for domain nucleation and lead to a higher switching speed. This effect is largest for samples where the overall nucleation barrier is high and where reversal takes place mainly by domain wall propagation. The influence of domain wall stray fields can therefore be modified by changing the substrate topography, and can be used to manipulate local switching speeds and switching reproducibility.

We thank A. Vaurès for sample preparation. Financial support by EU (BESSY-EC-HPRI contract No. HPRI-1999-CT-00028) and the Laboratoire Européen Associé "Mesomag" is gratefully acknowledged. J.C., F.R. and J.V. acknowledge partial financial support for personnel exchange by the "Acciones Integradas-Picasso" Programme, through Grant No. HF2003-0173.

[1] M. N. Baibich, J. M. Broto, A. Fert, F. Nguyen Van Dau, F. Petroff, P. Etienne, G. Creuzet, A. Friederich, and J. Chazelas, Phys. Rev. Lett. **61**, 2472 (1988).
[2] G. Binasch, P. Grünberg, F. Saurenbach, and W. Zinn, Phys. Rev. B **39**, 4828 (1989).
[3] E. B. Myers, D. C. Ralph, J. A. Katine, R. N. Louie, and R. A. Buhrman, Science **285**, 867 (1999).
[4] W. Weber, S. Riesen, and H. C. Siegmann, Science **291**, 1015 (2001).
[5] L. Néel, C. R. Hebd. Seances Acad. Sci. **255**, 1676 (1962).
[6] Y. Pennec, J. Camarero, J. C. Toussaint, S. Pizzini, M. Bonfim, F. Petroff, W. Kuch, F. Offi, K. Fukumoto, F. Nguyen Van Dau, and J. Vogel, Phys. Rev. B **69**, 180402(R) (2004).
[7] L. Thomas, M. G. Samant, and S. S. P. Parkin, Phys. Rev. Lett. **84**, 1816 (2000).
[8] R. Schäfer, R. Urban, D. Ullmann, H. L. Meyerheim, B. Heinrich, L. Schultz, and J. Kirschner, Phys. Rev. B **65**, 144405 (2002).
[9] W. Kuch, L. I. Chelaru, K. Fukumoto, F. Porrati, F. Offi, M. Kotsugi, and J. Kirschner, Phys. Rev. B **67**, 214403 (2003).
[10] V. Christoph and R. Schäfer, Phys. Rev. B **70** 214419 (2004).
[11] S. Wiebel, J.-P. Jamet, N. Vernier, A. Mougin, J. Ferré, V. Baltz, B. Rodmacq, and B. Dieny, Appl. Phys. Lett. **86**, 142502 (2005).
[12] J. Vogel, W. Kuch, R. Hertel, J. Camarero, K. Fukumoto, F. Romanens, S. Pizzini, M. Bonfim, F. Petroff, A. Fontaine, and J. Kirschner, Phys. Rev. B **72**, 220402(R) (2005).
[13] M. Sussiau, Ph.D. thesis, Université Paris Sud (1997).
[14] J. Vogel, W. Kuch, J. Camarero, K. Fukumoto, Y. Pennec, M. Bonfim, S. Pizzini, F. Petroff, A. Fontaine, and J. Kirschner, J. Appl. Phys. **95**, 6533 (2004).
[15] J. Stöhr, J. Magn. Magn. Mater. **200**, 470 (1999).
[16] H. Wende, Rep. Prog. Phys. **67**, 2105 (2004).
[17] C.M. Schneider, G. Schönhense, Rep. Prog. Phys. **65**, 1785 (2002).
[18] W. Kuch, Phys. Scr. **T109**, 89 (2004).
[19] M. Bonfim, G. Ghiringhelli, F. Montaigne, S. Pizzini, N.B. Brookes, F. Petroff, J. Vogel, J. Camarero, and A. Fontaine, Phys. Rev. Lett. **86**, 3646 (2001).
[20] J. Vogel, W. Kuch, M. Bonfim, J. Camarero, Y. Pennec, F. Offi, K. Fukumoto, J. Kirschner, A. Fontaine, and S. Pizzini, Appl. Phys. Lett. **82**, 2299 (2003).
[21] B. Raquet, M. Ortega, M. Goiran, A. R. Fert, J. P. Redoules, R. Mamy, J. C. Ousset, A. Sdaq, and A. Khmou, J. Magn. Magn. Mater. **150**, L5 (1995).
[22] J. Camarero, Y. Pennec, J. Vogel, M. Bonfim, S. Pizzini, M. Cartier, F. Ernult, F. Fettar, and B. Dieny, Phys. Rev. B **64**, 172402 (2001).
[23] B. Raquet, R. Mamy, and J. C. Ousset, Phys. Rev. B **54**, 4128 (1996).
[24] F. Romanens, S. Pizzini, J. Sort, F. Garcia, J. Camarero, F. Yokaichiya, Y. Pennec, J. Vogel, and B. Dieny, Eur. Phys. J. B **45**, 185 (2005).
[25] J. Moritz, B. Dieny, J.P. Nozières, Y. Pennec, J. Camarero, and S. Pizzini, Phys. Rev. B **71**, 100402(R) (2004).
[26] H.W. Schumacher, C. Chappert, R.C. Sousa, P.P. Freitas, and J. Miltat, Phys. Rev. Lett. **90**, 017204 (2003).
[27] W.E. Bailey, L. Cheng, D.J. Keavney, C.-C. Kao, E. Vescovo, and D.A. Arena, Phys. Rev. B **70**, 172403 (2004).

[28] B.C. Choi, J. Ho, G. Arnup, and M.R. Freeman, Phys. Rev. Lett. **95**, 237211 (2005).
[29] A. Krasyuk, F. Wegelin, S.A. Nepijko, H.J. Elmers, G. Schönhense, M. Bolte, and C.M. Schneider, Phys. Rev. Lett. **95**, 207201 (2005).
[30] E. Fatuzzo, Phys. Rev. **127**, 1999 (1962).
[31] M. Labrune, S. Andrieu, F. Rio, and P. Bernstein, J. Magn. Magn. Mater. **80**, 211 (1989).
[32] K. Fukumoto, W. Kuch, J. Vogel, F. Romanens, S. Pizzini, J. Camarero, M. Bonfim, and J. Kirschner, Phys. Rev. Lett. **96**, 097204 (2006).
[33] A. Hubert and R. Schäfer, *Magnetic Domains: The Analysis of Magnetic Microstructures*, Springer-Verlag, Berlin (1998).
[34] S. Bodea, W. Wulfhekel, and J. Kirschner, Phys. Rev. B **72**, 100403(R) (2005).